Effects of TRH on heteromeric rat erg1a/1b K^+ channels are dominated by the rerg1b subunit

Niklas M. Kirchberger, Iris Wulfsen, Jürgen R. Schwarz and Christiane K. Bauer

Institut für Angewandte Physiologie, Zentrum für Experimentelle Medizin, Universitätsklinikum Hamburg-Eppendorf, Universität Hamburg, D-20246 Hamburg, Germany

The erg1a (HERG) K^+ channel subunit and its N-terminal splice variant erg1b are coexpressed in several tissues and both isoforms have been shown to form heteromultimeric erg channels in heart and brain. The reduction of erg1a current by thyrotropin-releasing hormone (TRH) is well studied, but no comparable data exist for erg1b. Since TRH and TRH receptors are widely expressed in the brain, we have now studied the different TRH effects on the biophysical properties of homomeric rat erg1b as well as heteromeric rat erg1a/1b channels. The erg channels were overexpressed in the clonal somatomammotroph pituitary cell line GH_3/B_6, which contains TRH receptors and endogenous erg channels. Compared to rerg1a, homomeric rerg1b channels exhibited not only faster deactivation kinetics, but also considerably less steady-state inactivation, and half-maximal activation occurred at about 10 mV more positive potentials. Coexpression of both isoforms resulted in erg currents with intermediate properties concerning the deactivation kinetics, whereas rerg1a dominated the voltage dependence of activation and rerg1b strongly influenced steady-state inactivation. Application of TRH induced a reduction of maximal erg conductance for all tested erg1 currents without effects on the voltage dependence of steady-state inactivation. Nevertheless, homomeric rerg1b channels significantly differed in their response to TRH from rerg1a channels. The TRH-induced shift in the activation curve to more positive potentials, the dramatic slowing of activation and the acceleration of deactivation typical for rerg1a modulation were absent in rerg1b channels. Surprisingly, most effects of TRH on heteromeric rerg1 channels were dominated by the rerg1b subunit.

(Resubmitted 9 November 2005; accepted after revision 5 December 2005; first published online 8 December 2005)
Corresponding author C. K. Bauer: Institut für Angewandte Physiologie, Zentrum für Experimentelle Medizin, Universitätsklinikum Hamburg-Eppendorf, Martinistraße 52, D-20246 Hamburg, Germany.
Email: c.bauer@uke.uni-hamburg.de

Native *ether-à-go-go*-related gene (erg) K^+ currents were first described in the heart in sinoatrial node cells (Shibasaki, 1987). The cloning and identification of HERG as the human molecular correlate of the rapidly activating component (I_{Kr}) of the cardiac delayed rectifier current (Warmke & Ganetzky, 1994; Sanguinetti *et al.* 1995; Trudeau *et al.* 1995) allowed a detailed biophysical analysis of HERG channels, which confirmed the anomalous gating properties described by Shibasaki (1987). HERG channels exhibit inactivation kinetics that are faster than activation and recovery from inactivation that is faster than deactivation resulting in the observed functional inward rectification of erg currents (Spector *et al.* 1996; Wang *et al.* 1997). The use of specific blockers of erg channels allowed the isolation of the endogenous erg current, I_{Kr}, as a drug-sensitive current (Sanguinetti & Jurkiewicz, 1990) and revealed gradual differences mainly concerning the deactivation kinetics between the endogenous I_{Kr} and heterologously expressed HERG channels (reviewed in Bauer & Schwarz, 2001).

In 1997 it was reported that a splice variant of erg1 (= erg1a), named erg1b, had been cloned from heart (Lees-Miller *et al.* 1997; London *et al.* 1997). Erg1b lacks most of the HERG N-terminus (amino acids 1–376) and exhibits instead a much shorter and unique N-terminal sequence of 36 amino acids. The EAG or PAS domain in the distal N-terminus of erg1a channels plays a crucial role in their characteristic slow deactivation (Schönherr & Heinemann, 1996; Spector *et al.* 1996; Wang *et al.* 1998), and its absence in erg1b readily explains the observed much faster deactivation kinetics of erg1b currents (Lees-Miller *et al.* 1997; London *et al.* 1997). Differences in HERG and I_{Kr} deactivation kinetics have therefore been suggested to arise from heteromeric erg1 channels formed by coexpressed erg1a and -1b subunits in cardiac tissue (Lees-Miller *et al.* 1997; London *et al.* 1997). The

 DOI: 10.1113/jphysiol.2005.101667

presence of native erg1a/1b heteromeric channels in heart has recently been confirmed by coimmunoprecipitation studies (Jones *et al.* 2004).

Coexpression of erg1a and erg1b transcripts occurs not only in the heart, but also in smooth muscle (Ohya *et al.* 2002), different tumour cell lines (Crociani *et al.* 2003), pituitary and brain tissue (Hirdes *et al.* 2005). Recently, a detailed study showed that erg1a and erg1b are both widely expressed in adult mouse brain on the protein level (Guasti *et al.* 2005). The unexpected high expression of erg1b occurred always together with erg1a, and coassembly of the two isoforms has been demonstrated.

In contrast to erg1 (HERG or Kv11.1), the other two Kv11 family members erg2 and erg3 were described as being 'nervous system-specific' (Shi *et al.* 1997). In the rat (Saganich *et al.* 2001; Papa *et al.* 2003) and mouse brain (Guasti *et al.* 2005), there exists a partially overlapping expression of the different erg channel subunits, and they are also coexpressed in peripheral sympathetic ganglia (Shi *et al.* 1997) and in the pituitary (Schäfer *et al.* 1999). In pituitary lactotroph cells, the erg current is important for the control of prolactin secretion (Bauer *et al.* 1999). The inhibition of the erg current by the hypothalamic peptide thyrotropin-releasing hormone (TRH) was the first example of a receptor-mediated modulation of erg channels (Bauer *et al.* 1990; Corrette *et al.* 1996; Schäfer *et al.* 1999). Similarly to normal pituitary lactotroph cells, clonal pituitary GH_3 and GH_3/B_6 cells possess TRH receptors which are functionally coupled to endogenous erg channels via G protein activation (Bauer *et al.* 1990; Barros *et al.* 1992, 1993; Miranda *et al.* 2005). The TRH-induced reduction of the endogenous erg current and erg1a current induced by heterologous expression involves a shift in the voltage dependence of activation to more positive potentials, a slowing of activation kinetics, an acceleration of deactivation and a reduction of the maximally available erg current (Bauer *et al.* 1990; Bauer, 1998; Barros *et al.* 1998; Schledermann *et al.* 2001).

Recently, the proximal part of the HERG1a N-terminus has been found to be important for most TRH effects using HERG1a deletion mutants coexpressed with TRH receptors in *Xenopus* oocytes (Gomez-Varela *et al.* 2003*a*). Since the respective N-terminal domain is missing in erg1b, we have now investigated the TRH modulation of rerg1b and heteromeric rerg1a/1b channels expressed in GH_3/B_6 cells. These cells have previously been used as an expression system to study the TRH effects on erg1a, erg2 and erg3 channels and the underlying signal cascade (Schledermann *et al.* 2001). This approach combined the advantage of large erg currents due to channel overexpression with the advantage of an intact and physiologically relevant signal cascade.

Our present results show that the TRH effects on rerg1b clearly differ from those on rerg1a in the changes of their biophysical properties. Most interestingly, the data indicate that the rerg1b subunit is able to transfer its different sensitivity to TRH to heteromeric rerg1a/1b channels. The high expression levels of erg1a and erg1b in the brain (Guasti *et al.* 2005) combined with the fact that TRH receptors and TRH are present in most brain regions (reviewed in Sun *et al.* 2003) suggest that transmitter effects of TRH on heteromeric erg1a/1b channels also occur *in vivo* in the central nervous system.

Part of this work has been published in abstract form (Kirchberger *et al.* 2005).

Methods

Cell culture

Clonal rat somatomammotroph pituitary (GH_3/B_6) cells were cultured in Ham's F10 medium (Sigma, Deisenhofen, Germany) supplemented with 15% horse serum (Gibco, Karlsruhe, Germany), 2.5% fetal calf serum (Biother, Kelkheim, Germany) and 0.5% L-glutamine (Sigma). Culture medium was changed every 2–3 days. The cells were grown at 37°C in an atmosphere of 95% air and 5% CO_2 and passaged every 5–7 days.

Heterologous expression

Microinjection. GH_3/B_6 cells were plated onto poly-D-lysine-coated round glass coverslips in 35 mm plastic culture dishes (Nunc). Five to 15 h prior to the electrophysiological measurements, cells were injected (Eppendorf Transjector 5246) with cDNA coding for rat erg1a (10 ng μl^{-1}; Bauer *et al.* 1998; Acc. no. Z96106) or rat erg1b (30 ng μl^{-1}; Hirdes *et al.* 2005; Acc. no. AY669863). In coexpression experiments, rerg1a and rerg1b cDNA were coinjected either in a ratio of 1 : 3 (10 + 30 ng μl^{-1}) or 2 : 1 (20 + 10 ng μl^{-1}). To allow the detection of erg channel expressing cells, EGFP was coexpressed, or either rerg1a or rerg1b tagged with EGFP at the C-terminus was used for electrophysiological experiments. No differences were detected in the resulting erg currents mediated by tagged erg channels from those mediated by untagged erg channels with respect to activation curves, deactivation kinetics and modulation by TRH. To assess the formation of heteromeric rerg1a/1b channels, cDNA encoding dominant-negative rat erg1a G630S (Wimmers *et al.* 2001) constructed according to HERG G628S (Sanguinetti *et al.* 1996) was coinjected with EGFP-tagged rerg1b in GH_3/B_6 cells.

EGFP and DsRed tagging of rerg1a and rerg1b. Using PCR technique, the stop codon and the 3′-non-coding region of rerg1a and rerg1b were exchanged for the sequence TACTCTAGA, inserting an *Xba*I site

downstream of the mutated stop codon. These mutated rerg1a and rerg1b cDNAs were cloned into the pcDNA3.1 vector (Invitrogen, Karlsruhe, Germany). For the in-frame insertion of the EGFP-N1 (Invitrogen) and DsRed (BD Bioscience) cDNAs into the rerg1a and rerg1b constructs, new restriction sites were introduced by PCR technique. At the 5′ end an *Xba*I site and at the 3′ end an *Sfu*I site were introduced into EGFP-N1 and DsRed cDNA. The EGFP-N1 and the DsRed constructs were cloned into the pcDNA3.1/rerg1a and into the pcDNA3.1/rerg1b clone using the restriction sites *Xba*I and *Sfu*I.

Detection of EGFP and DsRed fluorescence. Fluorescent dyes were detected using an UV lamp (HBO50; Zeiss, Göttingen, Germany) and Zeiss filter sets '10' and '00' for EGFP and DsRed, respectively. Micrographs were taken with a Zeiss AxioCam camera in combination with the AxioVision software.

RT-PCR of GH_3/B_6 cells and brain

Animal care and experimental procedures were in accordance with the guidelines laid down by the animal welfare committee of the University of Hamburg. The brain of a femal Wistar rat was removed immediately after killing the animal by decapitation under halothane anaesthesia (Willy Rüsch GmbH, Kernen, Germany). RNAs were extracted from GH_3/B_6 cell cultures and the freshly prepared brain tissue using RNAzol™ B (AGS, Heidelberg, Germany). DNase digestion was performed before preparing cDNA. One microgram of total RNA was employed for oligo (dT) primed reverse transcription using M-MLV reverse transcriptase (Invitrogen). The cDNAs were amplified with 1.25 U of Taq DNA polymerase (Stratagene, Amsterdam, Netherlands), 1.5 mM $MgCl_2$, 0.2 mM of each dNTP in 50 μl reaction assays using 5 pmol of forward and reverse oligonucleotide primers specific for the different rerg1 splice variants. For amplification a predenaturation step at 94°C for 1 min was used followed by 40 cycles consisting of three temperature steps (first step: 94°C; second step: annealing temperature different for each primer pair; third step: 72°C; each temperature step lasted for 1 min) terminated by an elongation step at 72°C for 5 min. The annealing temperature was calculated for every primer pair from the G/C and A/T content of the oligonucleotide primers used in the reaction. A second amplification using nested primers was performed to check for weak amplification. In the PCRs with nested primers 1/50 of the amplification product of the first reaction was used as template in the second PCR. Amplified DNA fragments were analysed by agarose gel electrophoresis and sequencing. The following oligonucleotide primer sequences for the PCR amplifications were used.

rerg1a: nucleotides 1–353 (first amplification; accession no. Z96106):
Forward 5′ATGCCGGTGCGGAGGGGCCA3′
Reverse 5′TCATTCTTCACGGGCACCAC3′
Nucleotides 23–330 (second amplification):
Forward 5′TCGCGCCGCAGAACACCTTC3′
Reverse 5′CACCAAACACAGGAAGCAGC3′
rerg1b: nucleotides 1–754 (first amplification; accession no. AY669863):
Forward 5′ATGGCGATTCCAGCCGGGAA3′
Reverse5′GGTCGCCCAAGTTGTGCAGC3′
Nucleotides 22–754 (second amplification):
Forward 5′GAGAGCAGGACAGGGGCTCT3′
Reverse5′GGTCGCCCAAGTTGTGCAGC3′

Solutions

The standard pipette solution contained (mM): 140 KCl, 2 $MgCl_2$, 1 $CaCl_2$, 2.5 EGTA, 10 Hepes (about 66 nM free Ca^{2+}; EQCAL Biosoft, Cambridge, UK). pH was adjusted to 7.3 with KOH. For perforated-patch whole-cell experiments, nystatin (dissolved in DMSO) was added to the standard pipette solution with a final concentration of 0.24 mg ml^{-1}. For all experiments on heterologously expressed erg channels, the external solution contained (mM): 5 KCl, 135 NaCl, 4 $MgCl_2$, 1 $CaCl_2$, 10 glucose, 10 Hepes, 2.5 EGTA, 0.2 $NiCl_2$ (EQCAL: 75 nM free Ca^{2+}); pH was adjusted to 7.3 with NaOH; 500 nM tetrodotoxin (TTX) was added to the external solution. To study the dose-dependent modulation of the endogenous erg current in GH_3/B_6 cells by TRH, the external K^+ concentration was increased (iso-KCl solution) by replacing the whole amount of NaCl by KCl. In this external iso-KCl solution, pH was adjusted to 7.3 with KOH. Thyrotropin-releasing hormone (TRH) and the erg channel blocker E-4031 were diluted in external solution to yield a final concentration of 1 and 10 μM, respectively, when not stated otherwise. E-4031 was a generous gift from Eisai (Tokyo, Japan), TTX was purchased from Calbiochem (Bad Soden, Germany) and the other chemicals were from Sigma.

Electrophysiology and evaluation

In nystatin perforated-patch experiments (Horn & Marty, 1988), recording of whole-cell membrane currents was started when the series resistance settled between 8 and 30 MΩ. Series resistance errors were compensated as high as possible (about 60% in perforated-patch experiments, and 70–80% in conventional whole-cell experiments). When filled with intracellular solution, the pipette resistance varied between 3.5 and 4.5 MΩ. Fast and slow capacitances were compensated prior to the pulse protocols. The erg currents were isolated from other currents as difference currents before and after

selective pharmacological block. The data shown have not been corrected for the liquid junction potential (4.3 mV). All experiments were performed at room temperature. Stimulation, data acquisition and analysis were carried out using the Pulse/PulseFit 8.11 software in combination with an EPC-9 patch-clamp amplifier (HEKA, Lambrecht, Germany). Further data processing was performed with Excel (Microsoft, USA) and Igor Pro 4.04 (Wavemetrics, Lake Oswego, OR, USA). Significance was tested either with Student's two-tailed unpaired or paired *t* test and errors indicate S.E.M.

Results

TRH modulation of native GH_3/B_6 cell erg currents

For all experiments on the TRH-induced modulation of erg channels, membrane currents were recorded with the nystatin-perforated-patch technique to preserve the constituents of the TRH signal cascade as previously described (Barros *et al.* 1992; Schledermann *et al.* 2001). In most studies dealing with TRH effects on erg channels, TRH was used in a final concentration of 1 μM. We have now investigated the dose dependence of the TRH-induced shift in the voltage dependence of erg channel activation since this TRH effect occurs consistently in GH_3/B_6 cells with the endogenous erg current (Bauer *et al.* 1990) as well as with overexpressed rat and human erg1a, rat erg2 and erg3 channels (Schledermann *et al.* 2001). Due to the small density of the endogenous erg currents, membrane currents were recorded in iso-KCl as external solution and the erg current was isolated from other endogenous currents as E-4031-sensitive current (Fig. 1*A*) as previously described (Weinsberg *et al.* 1997). The voltage dependence of erg channel activation was studied with a double-pulse protocol. Starting from a holding potential of −80 mV at which erg channels are completely deactivated, 5 s variable depolarizing test pulses were applied followed by a hyperpolarization to −100 mV. The voltage dependence of erg channel activation was determined from the maximal amplitude of the transient erg inward current elicited upon the constant hyperpolarization following the variable test pulses (Fig. 1*Ac* and *B*). Current increase mirrors the process of recovery from inactivation and the subsequent decay is due to erg channel deactivation. In Fig. 1*B*, the mean normalized erg current amplitudes before and after application of 100 nM TRH were plotted *versus* the potential of the preceding test pulses. The resulting data points were fitted with a Boltzmann equation yielding the potentials for half-maximal isochronal (5 s) activation ($V_{0.5}$) of the erg channels. After TRH application, the $V_{0.5}$ value was shifted by 18.3 ± 2.0 mV ($n = 4$) from -30.0 ± 2.8 mV to -11.7 ± 1.0 mV. The dose–response relation given in Fig. 1*C* shows that 1 μM TRH induced a similar shift (18.7 ± 1.8 mV, $n = 4$) in the erg activation curve to more depolarized potentials. Also the concentration of 10 nM TRH was able to affect the voltage dependence of activation, although the amount of the shift was smaller (10.2 ± 3.9 mV, $n = 4$) and erg current reduction occurred with considerably slower time course and with longer latency compared to experiments with 100 nM or 1 μM TRH concentrations, where erg current reduction was normally achieved within 3 min after TRH application. To minimize erg current reduction due to run-down effects in the course of long-lasting experiments, erg activation curves were determined not later than 10 min after TRH application. Therefore, it cannot be completely excluded that 1 nM TRH would exert an effect on the erg current after prolonged exposure.

The endogenous erg current in GH_3/B_6 cells strongly resembles rerg1a current measured under comparable conditions (Bauer *et al.* 1998). Nevertheless, GH_3/B_6 cells express mRNA for rerg1 and rerg2 (Wulfsen *et al.* 2000). In these PCR experiments, C-terminal primers have been used which do not distinguish between N-terminal splice variants. To investigate whether rerg1b channels might contribute to the endogenous erg current, we performed RT-PCRs of GH_3/B_6 cells with primers specific for rerg1a and rerg1b. Figure 1*D* shows that even in the second round of amplification, no transcripts of rerg1b were detected, whereas transcripts of rerg1a were obvious already after the first amplification. Rat brain tissue served as a positive control for rerg1a and rerg1b.

Overexpression of rerg channels in GH_3/B_6 cells

A striking property of erg channels is the paradoxical increase in conductance in elevated $[K^+]_e$ (Shibasaki, 1987; Lees-Miller *et al.* 1997; Sturm *et al.* 2005). We took advantage of this property by measuring the endogenous erg current in iso-KCl (Fig. 1). As illustrated in Fig. 2*A* and *B*, the native erg current is hardly detectable in an external solution with physiological 5 mM K^+. Therefore, the E-4031-sensitive current recorded in 5 mM K^+ in GH_3/B_6 cells previously injected with erg cDNA is regarded as representing almost exclusively current mediated by the heterologously expressed erg channels.

In the following experiments, E-4031-sensitive membrane currents were recorded 5–8 h after cDNA injection from erg channel expressing GH_3/B_6 cells identified by their EGFP fluorescence. Since injection of the same concentration of rerg1b cDNA as rerg1a cDNA resulted in drastically smaller amplitudes of rerg1b compared to rerg1a currents, the injected cDNA coding for rerg1b channels had 3 times the concentration of rerg1a cDNA to yield analysable rerg1b currents. (Fig. 2*A* and *B*).

The formation of heteromeric rerg1a/1b channels in GH_3/B_6 cells was investigated by the use of the dominant-negative mutant rerg1aG630S. To assess the

percentage of functional homomeric rerg1b channels upon coexpression with rerg1a, erg current amplitudes were determined after the expression of different combinations and ratios of rerg1a and rerg1b channel subunits. The average of the maximum erg outward current amplitude as well as of the peak inward current amplitude at −100 mV measured with an activation protocol are summarized in Fig. 2*B*. Coinjection of rerg1aG630S/rerg1b with a cDNA ratio 2 : 1 resulted in drastically decreased erg current amplitudes. The mean inward erg current which could be determined quite accurately despite its small amplitude amounted to 5% of the mean erg current amplitude resulting from the corresponding coexpression of WT-rerg1a/rerg1b. In the ratio 1 : 3, rerg1aG630S coexpression with rerg1b still resulted in a clearly reduced amplitude of erg currents which amounted to 13% of the corresponding mean WT-rerg1a/rerg1b inward current amplitude and to 47% of the rerg1b current amplitude recorded after injecting the same concentration of rerg1b cDNA alone. The rerg1aG630S/rerg1b (ratio 1 : 3) erg current resembled homomeric rerg1b current with respect to their fast deactivation kinetics, suggesting that native erg channel subunits did not considerably contribute to these small amplitude erg currents.

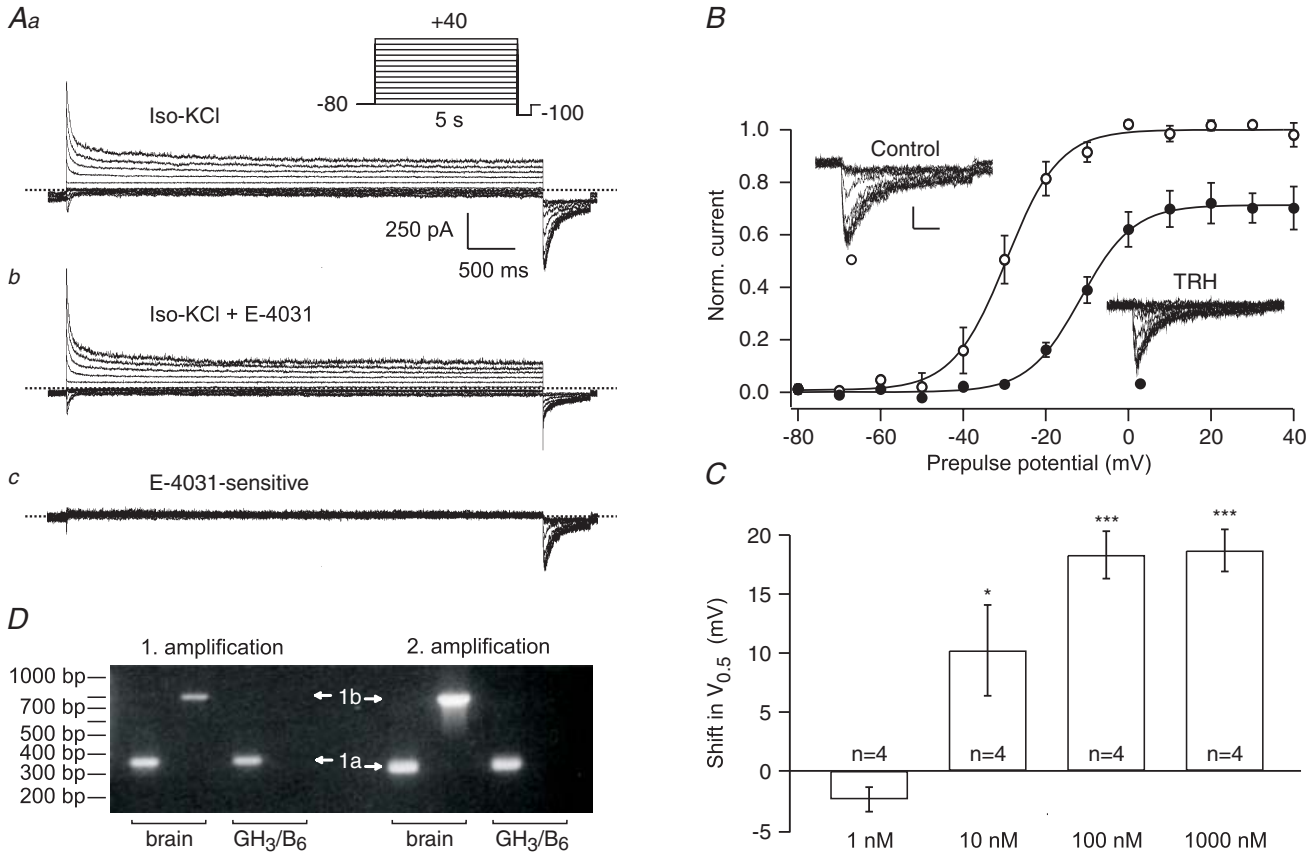

Figure 1. Modulation of GH_3/B_6 cell erg currents by TRH
Membrane currents were recorded in native GH_3/B_6 cells in the perforated-patch whole-cell configuration using isotonic KCl as external solution. From a holding potential of −80 mV, erg current activation was measured with 5 s depolarizing pulses to potentials between −80 and +40 mV followed by a constant hyperpolarizing pulse to −100 mV. The erg currents (*Ac*) were isolated as difference between the current traces recorded before (*Aa*) and after application of 10 μM E-4031 (*Ab*). *B*, mean normalized maximal erg current amplitudes elicited at repolarization to −100 mV as a function of the preceding test pulse potential before (○) and after (●) the application of 100 nM TRH. Data points were fitted with Boltzmann equations yielding the potentials of half-maximal activation ($V_{0.5}$). Scale bars, valid for current traces in both insets, denote 100 pA and 100 ms. *C*, shift in $V_{0.5}$ values of erg currents induced by the application of different concentrations of TRH. Number of experiments indicated, error bars denote S.E.M.; * and *** denote significant differences before and after TRH with $P \leq 0.05$ and $P \leq 0.001$, respectively; one-tailed paired *t* test. *D,* GH_3/B_6 cells express transcripts for rat erg1a, but not for erg1b. RT-PCR amplification products from the first and second round of amplification are shown. 20% (1 amplification, left side) or 10% (2 amplification, right side) of the PCR products were separated on a 1.5% agarose gel. Tissue origin of cDNAs used in the PCR reactions: rat brain (lanes 1, 2, 5, 6), GH_3/B_6 cells (lanes 3, 4, 7, 8). Amplification products of rat erg1a (1a) or rat erg1b (1b) are marked by arrows.

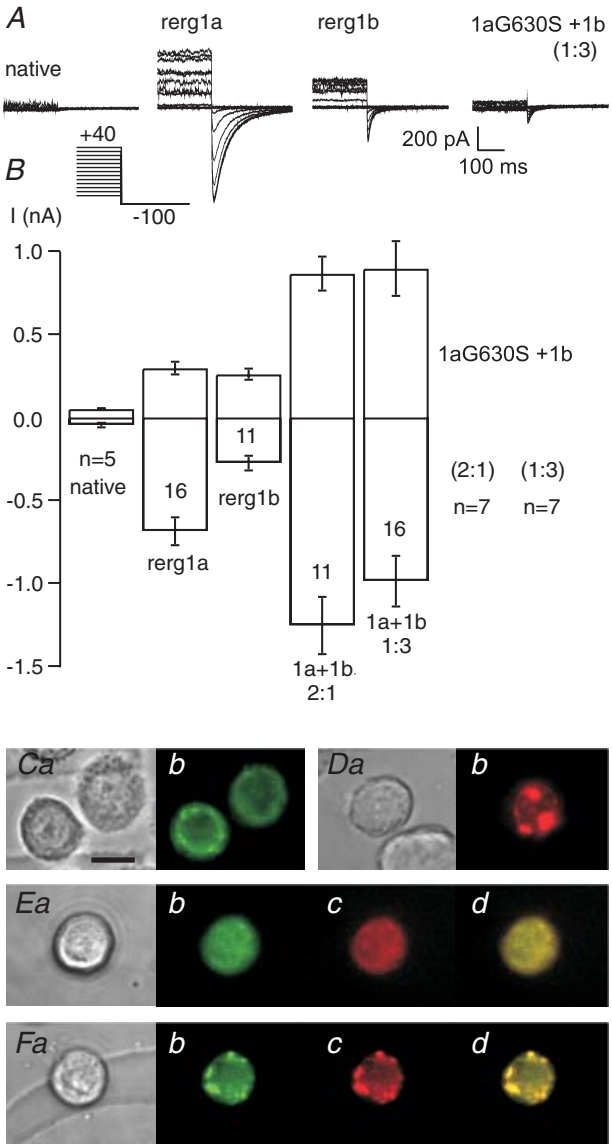

Figure 2. Coexpressed rat erg1a and erg1b subunits form heteromeric channels in GH_3/B_6 cells
A, E-4031-sensitive currents recorded in external solution with 5 mM external K^+ in uninjected GH_3/B_6 cells and cells after injection of cDNA coding for rerg1a, rerg1b and coinjection of the dominant-negative rerg1a mutant rerg1aG630S with rerg1b. Depicted parts of current traces show families of erg currents recorded at the end of the 5 s depolarizing pulses followed by a hyperpolarization to −100 mV. The activation protocol started from a holding potential of −80 mV. *B*, amplitudes of outward and inward erg currents recorded in uninjected GH_3/B_6 cells (native) and GH_3/B_6 cells 5–8 h after injection of cDNA coding for rerg1a (10 ng μl^{-1}), rerg1b (30 ng μl^{-1}) and rerg1a + rerg1b in the ratios 2 : 1 (20 + 10 ng μl^{-1}) and 1 : 3 (10 + 30 ng μl^{-1}). Filled bars indicate experiments where the dominant-negative mutant rerg1aG630S instead of wild-type rerg1a was coexpressed with rerg1b. Data are means ± S.E.M. of maximum outward erg current amplitudes and of erg tail current amplitudes at −100 mV. Number of experiments indicated. *C–F*, bright field (*a*) and fluorescence (*b* and *c*) micrographs of GH_3/B_6 cells injected with cDNA coding for EGFP-tagged rerg1a (10 ng μl^{-1}, *C*), DsRed-tagged rerg1b (30 ng μl^{-1}, *D*) and EGFP-tagged rerg1a + DsRed-tagged rerg1b in the ratio 1 : 3 (10 + 30 ng μl^{-1}, *E* and *F*). *Ed* and *Fd* show merged rerg1a- and rerg1b-specific fluorescence. Scale bar: 10 μm.

Figure 2*B* also illustrates that the rerg1a inward current amplitudes were clearly larger than the corresponding outward current amplitudes, whereas the inward and outward current amplitudes for rerg1b were approximately the same. The different ratios of maximum sustained erg outward current to the absolute erg tail current amplitude measured at −100 mV can be used as a measure of inward rectification strength. Rerg1b exhibited a much higher relative outward current amplitude (1.08 ± 0.15, $n = 11$) than rerg1a (0.44 ± 0.03, $n = 16$, $P \leq 0.0001$). The relative outward current amplitude was also significantly increased compared to rerg1a upon coexpression of rerg1a with rerg1b in the ratios 2 : 1 (0.71 ± 0.05, $n = 11$, $P \leq 0.0001$) and 1 : 3 (0.87 ± 0.04, $n = 16$, $P \leq 0.0001$).

To visualize and compare the subcellular distribution of the two rerg1 subunits, we injected cDNA coding for EGFP-tagged rerg1a and DsRed-tagged rerg1b channel subunits in GH_3/B_6 cells. In most cells injected either with rerg1a or with rerg1b cDNA, rerg1a showed a more homogeneous cellular distribution than rerg1b which often exhibited strong intracellular clustering (Figs 2*C* and *D*). In these experiments, no fluorescent signals were detected with the corresponding other filter set. Upon coinjection of cDNA coding for rerg1a and rerg1b, an identical cellular distribution of the two channel subunits was consistently observed (Figs 2*E* and *F*). Most coinjected GH_3/B_6 cells exhibited a diffuse rerg expression pattern, but clustering of rerg channels also occurred in some cells (Fig. 2*F*). The same results were obtained with DsRed-coupled rerg1a and EGFP-tagged rerg1b channel subunits.

Modulation of overexpressed rat erg1a and erg1b channels by TRH in GH_3/B_6 cells

Membrane currents of GH_3/B_6 cells previously injected with cDNA coding for rerg1a or rerg1b K^+ channel subunits were recorded in external solution with 5 mM K^+ with the nystatin-perforated-patch technique. The final TRH concentration used in these experiments was always 1 μM to guarantee maximal and fast activation of the signal cascade relevant for the modulation of erg channels. The same experiments were performed after coexpression of rerg1a with rerg1b in the ratio 1 : 3 and also in the ratio 2 : 1 to assess whether gradual differences could be observed in the TRH effects. Independent of the type of rerg1 isoform expressed in GH_3/B_6 cells, TRH induced a clear reduction of the outward and inward erg currents. The erg current reduction was usually complete within 3–5 min. This time course was comparable to that described for the TRH response of the endogenous erg current in GH_3/B_6 cells (Bauer *et al.* 1990 and the present study) and rat lactotrophs (Corrette *et al.* 1996; Schäfer *et al.* 1999) and erg1–3 channels overexpressed in GH_3/B_6 cells (Schledermann *et al.* 2001). TRH was permanently applied to the bath and no indications of a reversibility of the effects

on the erg current were observed during the experiments. To analyse the biophysical basis of the TRH-induced erg current reduction, different pulse protocols were applied before and after TRH application. The time course of the TRH response was always traced with a standard test pulse sequence. At the end of each experiment, all pulse protocols were repeated in the presence of E-4031 to enable the isolation of the specific erg currents by subtraction of the E-4031-resistant membrane currents.

TRH effects on the activation of differently composed rerg1 channels

The voltage dependence of rerg1a and rerg1b current activation before and after TRH application was investigated with 5 s depolarizing pulses from a holding potential of −80 mV (Fig. 3*A*). The decrease in the amplitudes of the E-4031-sensitive currents at the end of the depolarizing pulses occurring at more positive test potentials demonstrates the inward rectification of the erg channels (Fig. 3*Ba* and *b*). Control erg current amplitudes peaked at 0 mV for rerg1a and at +10 mV for rerg1b. A constant hyperpolarization to −100 mV followed the variable test pulses to determine the fraction of erg channels activated by the preceding depolarization. The control activation curves (Fig. 3*Ca* and *b*) of rerg1a and rerg1b exhibited a slightly different voltage dependence ($P \leq 0.0001$). Half-maximal activation was achieved at -15.8 ± 1.4 mV for rerg1a ($n = 16$) and at -4.2 ± 1.4 mV for rerg1b ($n = 14$).

TRH reduced the sustained rerg1a and rerg1b outward current (Fig. 3*Ba* and *b*) and induced a significant shift in the activation curve of rerg1a channels to more positive potentials (Fig. 3*Ca*). The mean shift in the inflection potentials was 10.0 ± 1.3 mV ($n = 16$, $P \leq 0.001$). In contrast, no significant shift in the inflection potentials was found for rerg1b (2.1 ± 1.4 mV, $n = 14$), but the reduction of the maximal available current was more pronounced ($P \leq 0.01$) for rerg1b (47.8 ± 4.0% current reduction) than for rerg1a (31.6 ± 4.1% current reduction).

The same experiments were performed after coexpression of rerg1a with rerg1b in two different cDNA concentration ratios. Interestingly, the $V_{0.5}$ values of the activation curves for coexpressed rerg1a and rerg1b channel subunits (-15.5 ± 1.8 mV, $n = 11$ and -14.9 ± 1.8 mV, $n = 14$, for the ratios of rerg1a to rerg1b of 2 : 1 and 1 : 3, respectively) were very similar to the half-maximal activation of rerg1a channels and differed significantly from that of rerg1b ($P \leq 0.0001$, for both ratios). Also in these experiments, TRH induced a clear reduction in the late outward current amplitude as well as in the maximal available erg inward current amplitude elicited upon the subsequent hyperpolarization (Fig. 3*Bc*, *Bd*, *Cc* and *Cd*). The amount of current reduction measured from the activation curves was 37.9 ± 4.3% and 42.9 ± 4.6% for the ratios of rerg1a to rerg1b of 2 : 1 and 1 : 3, respectively.

A small shift in the activation curves by *ca* 5 mV was found after TRH application for the rerg1a/1b ratio of 2 : 1 (4.6 ± 1.6 mV, $n = 11$, $P \leq 0.05$). In contrast, TRH induced no significant shift in the voltage dependence of erg channels formed after rerg1a and rerg1b cDNA injection in the ratio 1 : 3 (2.4 ± 1.3 mV, $n = 14$). Figure 3*D* illustrates that an involvement of rerg1b subunits in rerg1 channel formation inhibited the TRH-induced shift in the voltage dependence of activation, although the voltage dependence itself was determined by rerg1a channels.

TRH effects on the deactivation kinetics of erg currents

The time course of fast erg channel deactivation was determined from the activation protocols, and Fig. 4*A* again demonstrates the fast deactivation kinetics of rerg1b compared to rerg1a. The time constants of fast deactivation (τ_{deact}) were determined from the tail currents elicited upon the repolarization to −100 mV by fitting an exponential function to the fast decay phase of the erg currents. For each experiment, a mean time constant was obtained by averaging the time constants determined for the tail currents following depolarizing pulses to potentials between 40 and 10 mV which maximally activated the erg channels.

After coexpression of rerg1a and rerg1b, the resulting currents exhibited mean values for τ_{deact} which were significantly larger than τ_{deact} for rerg1b ($P \leq 0.001$, for both rerg1a : rerg1b ratios) and smaller than τ_{deact} determined for rerg1a ($P \leq 0.001$, for the rerg1a : rerg1b ratio of 1 : 3) under control conditions (Fig. 4*B*, white columns). Also the values for τ_{deact} for the two rerg1a : rerg1b ratios differed significantly from each other, suggesting that the ratio of injected rerg cDNA is correlated with the ratio of functionally expressed rerg1a and rerg1b channel subunits underlying the recorded erg currents.

The deactivation time course of rerg1a was significantly accelerated after the application of TRH. In contrast, the much faster deactivation kinetics of rerg1b were not significantly altered by TRH. Figure 4*B* shows that TRH induced a significant decrease in the time constants of fast deactivation of the different heteromeric rerg1 channels. Nevertheless, this acceleration (about 16% for both rerg1a : rerg1b ratios) was less pronounced than that observed in homomeric rerg1a channels (about 24%).

TRH effects on the activation kinetics of different rerg1 currents

The time course of erg current activation was assessed with an envelope-of-tail protocol (Fig. 5), using a test

pulse potential of +40 mV with variable duration. The amplitudes of the inward erg currents elicited by a subsequent hyperpolarization to −100 mV increased with prepulse duration. The time course of erg1b activation has previously been reported to involve more than one time constant (Lees-Miller *et al.* 1997). Since the data given in Fig. 5*B* were not well fitted with single exponential functions, we determined the prepulse duration at which

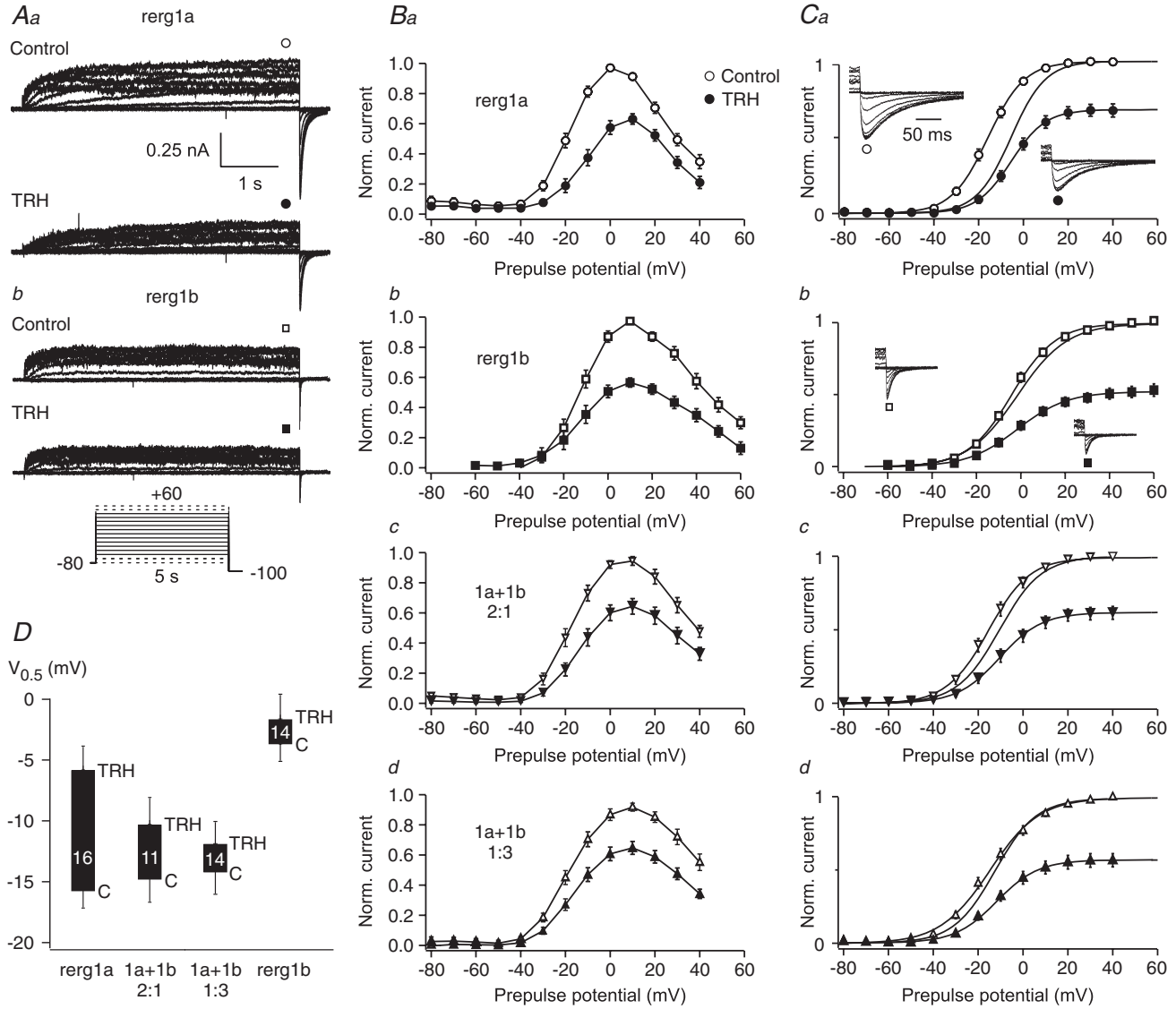

Figure 3. Rerg1b inhibits the TRH-induced shift in rerg1 activation curves
Membrane currents were recorded in the perforated-patch whole-cell configuration in GH_3/B_6 cells previously injected with erg cDNA before and after application of 1 μM TRH. Data from cells previously injected with erg cDNA coding for rerg1a (*a*), rerg1b (*b*) and rerg1a + rerg1b in the ratios 2 : 1 (*c*) and 1 : 3 (*d*). Erg currents were isolated as E-4031-sensitive currents. *A,* rerg1a (*Aa*) and rerg1b (*Ab*) currents elicited with 5 s depolarizing test pulses from a holding potential of −80 mV before and after application of TRH. The erg tail currents elicited upon repolarization to −100 mV are shown as insets on expanded time scale in *Ca* and *b*. *B,* mean (± S.E.M.) relative erg current amplitudes measured at the end of the depolarizing test pulses as indicated in *A*. Current amplitudes before (open symbols) and after (filled symbols) TRH application were normalized to the maximal control erg current amplitude. *C,* plots of the maximal erg current amplitude elicited with the constant hyperpolarizing pulse to −100 mV as a function of the preceding test pulse potential. Mean relative erg current amplitudes (means ± S.E.M.) are given before (open symbols) and after (filled symbols) TRH application, and the continuous lines represent Boltzmann functions fitted to the data points. In addition, the normalized activation curves after TRH application are shown to facilitate the comparison of their voltage dependence. *D,* comparison of the TRH-induced shift in the voltage dependence of erg current activation determined for the different erg1 currents. The mean $V_{0.5}$ values before (C: bottom of the columns) and after TRH application (TRH: top of the columns) are derived from Boltzmann functions fitted to the data points of single experiments. Downward error bars starting from the bottom of the columns indicate –S.E.M. of the control values, upward error bars starting from the top of the columns indicate +S.E.M. of the values after TRH application. Numbers indicate the number of experiments.

half-maximal erg tail current amplitude was obtained ($t_{0.5}$, see Gomez-Varela *et al.* 2003*a*).

Homomeric rerg1a and rerg1b channels differed in their activation kinetics under control conditions. At +40 mV, rerg1b activation was significantly faster ($t_{0.5}$: 116 ± 14 ms, $n = 11$, $P \leq 0.05$) than activation of rerg1a ($t_{0.5}$: 165 ± 10 ms, $n = 16$). TRH induced a prominent slowing of rerg1a activation kinetics by more than 90%. The magnitude of this effect was much smaller for rerg1b (slowing by 24%, $P \leq 0.05$). After coexpression of rerg1a and rerg1b in a ratio of 2 : 1, no significant differences from homomeric erg1a channels were observed in the activation kinetics under control conditions. Nevertheless, TRH induced a less pronounced slowing of the activation kinetics (by about 55%) leading to significantly smaller $t_{0.5}$ values after TRH ($t_{0.5}$: 238 ± 21 ms, $n = 11$) compared to rerg1a.

Coexpression of rerg1a and rerg1b in the ratio 1 : 3 resulted in rerg1 currents, which activated as fast as homomeric rerg1b channels under control conditions and also in the presence of TRH ($t_{0.5}$: 116 ± 13 ms and 143 ± 12 ms, respectively, $n = 14$). Thus, the TRH-induced increase in mean $t_{0.5}$ amounted only to 23% ($P \leq 0.05$).

TRH effects on steady-state inactivation and conductance of rerg1 channels

The voltage dependence of inactivation was studied with a triple-pulse protocol according to Smith *et al.* (1996) as shown in Fig. 6*A*. A 500 ms depolarization to +80 mV (P1) which completely activated and inactivated the erg channels was followed by 10 ms variable pulses to potentials between +80 and −140 mV (P2). The erg current amplitude at the subsequent depolarizing pulse to +40 mV (P3) was used to assess the proportion of erg channels which recovered from inactivation during P2. At more negative P2 test potentials, the erg current amplitude elicited with the P3 pulse declined due to deactivation during the P2 pulse. This effect was much more pronounced for the fast deactivating rerg1b current than for rerg1a (Fig. 6*B*). To account for this deactivation-induced decrease in P3 current amplitude, steady-state inactivation curves were obtained by sigmoidal fits to the data points in the potential ranges where no deactivation occurred. Before averaging the P3 erg current amplitudes measured in the individual experiments, amplitude values were normalized to the maximal current amplitude. The mean P3 current amplitudes were then used for the sigmoidal fits and the data were normalized again to the extrapolated maximal P3 erg current amplitudes before TRH application.

The inactivation curve determined for rerg1b is located at considerably more positive potentials compared to that of rerg1a ($V_{0.5}$ values: −73.7 mV for rerg1a, $n = 8$; −16.2 mV for rerg1b, $n = 8$; Fig. 6*B*). Coexpression of rerg1a with rerg1b in the ratio 1 : 3 resulted in erg currents which exhibited a voltage dependence of inactivation more similar to rerg1b than to rerg1a. The sigmoidal fit to the averaged data yielded a $V_{0.5}$ of −34.1 mV, $n = 6$.

Despite a more (rerg1b) or less (rerg1a) pronounced reduction of the erg current elicited with the P3 pulse, TRH produced no significant shift in the voltage dependence of the inactivation curves ($V_{0.5}$ values after TRH: −68.4 mV for rerg1a, −11.9 mV for rerg1b and −34.7 mV for rerg1a +1b).

To determine the TRH effect on the 'window conductance' for the two rerg1 isoforms and heteromeric rerg1a/1b channels, activation curves were obtained (as described for Fig. 3) before and after TRH application in the same set of experiments as used for the analysis of steady-state inactivation. Mean inflection potentials of activation curves before and after TRH application

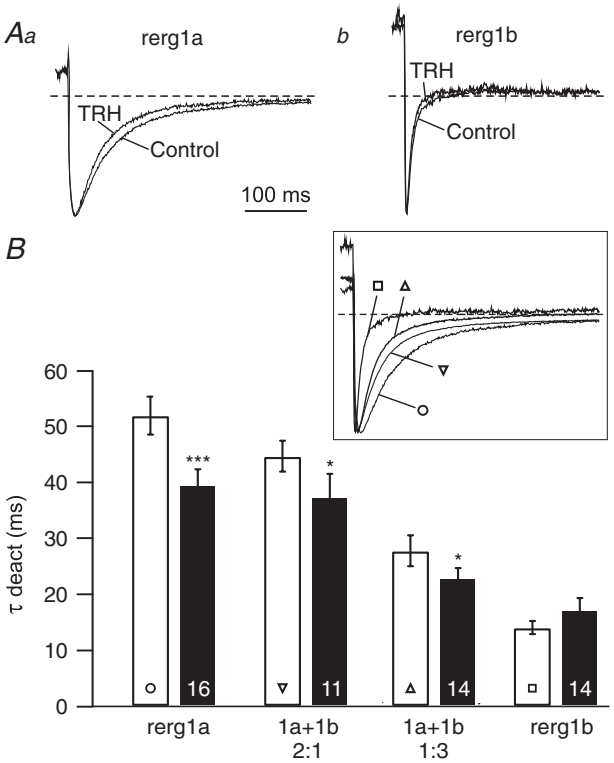

Figure 4. Different effects of TRH on erg deactivation kinetics
Analysis of deactivation kinetics using erg tail currents obtained from the same experiments as shown in Fig. 6. *A,* superimposed scaled rerg1a (*Aa*) and rerg1b (*Ab*) current traces before and after application of TRH. The erg currents were isolated with E-4031. *B,* mean time constants of fast deactivation at −100 mV before (open columns) and after application of TRH (filled columns) obtained in GH_3/B_6 cells injected with cDNA coding for rerg1a, rerg1a + rerg1b (ratio 2 : 1), rerg1a + rerg1b (ratio 1 : 3) and rerg1b. * and *** denote significant differences before and after TRH with $P \leq 0.05$ and $P \leq 0.001$, respectively; one-tailed paired *t* test. The inset shows superimposed scaled control erg tail currents.

were for rerg1a −17.0 mV and −8.3 mV, for rerg1b −5.2 mV and −8.3 mV, and for rerg1a +1b (ratio 1 : 3) −18.4 mV and −15.9 mV, respectively. These activation curves are included as lines in the graphs of Fig. 6*B*. Steady-state conductance was calculated by multiplying the fitted data of the respective normalized activation curves with those of the steady-state inactivation curves (Fig. 6*C*). Over the whole voltage range, the steady-state conductance was considerably larger for rerg1b than for rerg1a although the difference was especially pronounced in the more depolarized voltage range. This was mirrored by the relative peak values of the steady-state conductance, which amounted to 0.06 at −10.2 mV for rerg1a, and 0.23 at +5.2 mV for rerg1b. The erg channels formed by coexpressed rerg1a and rerg1b subunits exhibited considerably more steady-state conductance than homomeric rerg1a, although the conductance peaked with a value of 0.19 at a similar voltage (−9.1 mV) as the rerg1a steady-state conductance.

Although TRH clearly reduced the steady-state conductance for all tested rerg channels, this effect was most prominent for rerg1a in the lower voltage range. This is consistent with the TRH-induced shift in the rerg1a activation curve to more positive potentials.

To assess whether the relatively high series resistance error remaining after compensation in perforated-patch whole-cell experiments considerably affected the steady-state inactivation data obtained with the fast

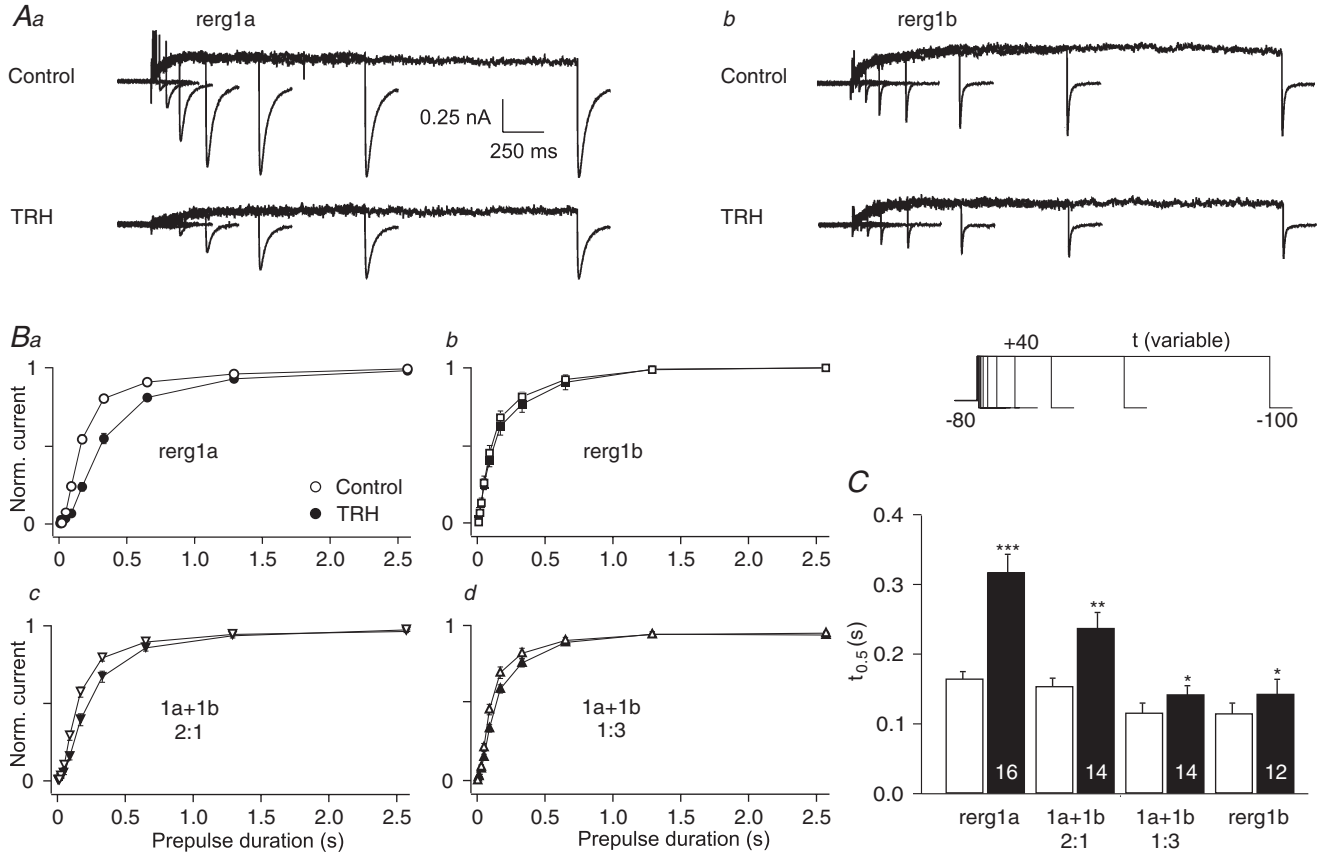

Figure 5. Coexpression of rerg1b inhibits the TRH-induced slowing of rerg channel activation
The time course of erg current activation was investigated before and after application of 1 μM TRH in GH_3/B_6 cells previously injected with erg cDNA. *A,* rerg1a and rerg1b current traces before and after TRH application evoked by depolarizing pulses to +40 mV of increasing duration followed by a hyperpolarization to −100 mV. The holding potential was −80 mV. The erg currents were isolated using E-4031 as specific blocker. *B*, maximal amplitudes of erg currents elicited upon the hyperpolarizations before (open symbols) and after (filled symbols) application of 1 μM TRH were normalized, averaged and plotted against the duration of the preceding depolarizing pulse. Data from cells previously injected with erg cDNA coding for rerg1a (*Ba*), rerg1b (*Bb*) and rerg1a + rerg1b in the ratios 2 : 1 (*Bc*) and 1 : 3 (*Bd*). *C,* comparison of the time to reach half-maximal activation ($t_{0.5}$) before (open columns) and after TRH application (filled columns) for the different rerg1 currents. Means ± S.E.M., number of experiments indicated; *, ** and *** denote significant differences before and after TRH with $P \leq 0.05$, $P \leq 0.01$ and $P \leq 0.001$, respectively; two-tailed paired *t* test.

triple pulse protocol, we performed some additional experiments in the conventional whole-cell configuration (lower access resistance and higher series resistance compensation). In these experiments, the values for half-maximal steady-state inactivation were −85.7 mV (rerg1a, $n = 3$), −22.8 mV (rerg1b, $n = 3$) and −37.9 mV (rerg1a/1b, ratio 1 : 3, $n = 2$), and thus between 12.0 and 3.9 mV more negative compared to the perforated-patch condition, but with essentially the same huge differences between the rerg1 isoforms. Also differences in the $V_{0.5}$ values of the activation curves were determined between perforated-patch and conventional whole-cell experiments, with 8–11 mV more negative $V_{0.5}$ values obtained in the conventional whole-cell experiments (data not shown). These deviations in the activation curves obtained with the different recording techniques in the

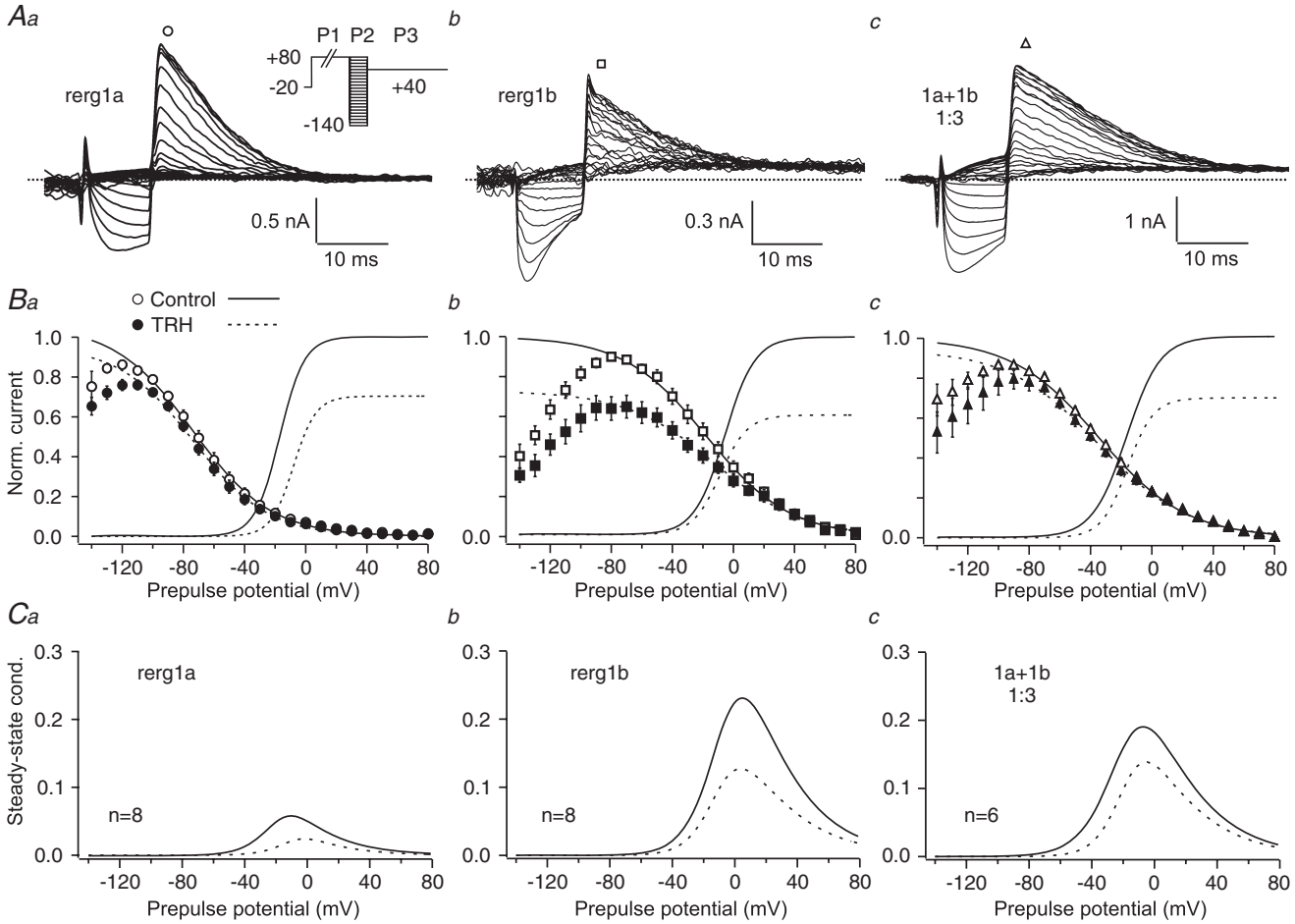

Figure 6. TRH reduces rat erg1 steady-state whole-cell conductance without altering the voltage dependence of steady-state inactivation

E-4031-sensitive currents were recorded in GH_3/B_6 cells previously injected with cDNA coding for rerg1a (*Aa*), rerg1b (*Ab*) and rerg1a + rerg1b in the ratio 1 : 3 (*Ac*) using a triple pulse protocol. The holding potential was −20 mV and a 500 ms prepulse to +80 mV (P1) preceded the pulse sequences to fully activate and inactivate the erg channels. To induce potential-dependent recovery from inactivation, 10 ms pulses to potentials between +80 and −140 mV (P2) were used. A subsequent 200 ms depolarization to +40 mV (P3) induced instantaneous erg outward currents and their amplitude mirrored the proportion of erg channels recovered during the preceding P2 pulses. *B,* P3 erg current amplitudes before (open symbols) and after application of TRH (filled symbols) for rerg1a (*Ba*), rerg1b (*Bb*) and rerg1a + rerg1b (*Bc*) plotted against the P2 potential. Data were normalized to the extrapolated maximal erg current amplitudes before TRH application obtained by sigmoidal fits to the data points in the potential ranges where no deactivation occurred during the P2 pulse. In addition to the inactivation curves, Boltzmann fits representing the activation curves before (continuous lines) and after (dashed lines) TRH application in the same sets of experiments are shown. Corresponding $V_{0.5}$ values are given in the text. *C,* voltage dependence of the steady-state erg conductance before (continuous lines) and after (dashed lines) TRH application obtained by multiplying the values of the normalized activation and steady-state inactivation curves given in *B*.

order of magnitude of 10 mV can at least partially be explained by the continued presence of a Donnan potential in the perforated-patch experiments.

Discussion

We investigated the TRH-induced changes in the biophysical properties of rat erg1a and erg1b channels as well as heteromeric erg channels formed by coexpressed rerg1a and rerg1b subunits. Anterior pituitary GH_3/B_6 cells served as an expression system to study the TRH-induced modulation of erg channels via activation of the endogenous signal cascade. The results show several distinct properties of rerg1b compared to rerg1a channels with respect to normal gating properties as well as to TRH effects. Coexpressed rerg1a and rerg1b subunits formed heteromeric erg channels. Depending on the investigated parameter, their properties were intermediate or dominated either by rerg1a or by rerg1b. Interestingly, rerg1b subunits seem to transfer their type of modulation by TRH to heteromeric rerg1a/1b channels.

GH_3/B_6 cells as expression system for the analysis of TRH-induced erg channel modulation

We have previously shown that GH_3/B_6 cells express transcripts for rerg1, and also transcripts for rerg2 were consistently detected in a second round of amplification (Wulfsen *et al.* 2000). The present result that rerg1a, but not the splice variant rerg1b, is expressed in these cells is in line with the fact that the native erg current resembles rerg1a (Bauer *et al.* 1998).

The unusually strong conductance increase with increasing external K^+ concentration, which is conserved in all three members of the erg family (Sturm *et al.* 2005), has been exploited for the use of GH_3/B_6 cells as an erg channel expression system. The native erg current was investigated in external iso-KCl solution, which maximized the erg current amplitude at more negative potentials. In contrast, after cDNA injection, erg currents resulting after erg cDNA injection were recorded in external solution containing a physiological K^+ concentration of 5 mM. In this low K^+ bath solution, the endogenous erg current was negligible compared to the erg current amplitude after overexpression of rerg1a and rerg1b channels. Therefore, the recorded total erg current was assumed to represent the properties of the newly expressed erg channels.

The concentration dependence of the TRH effect was investigated in the native erg current. Using the TRH-induced shift in the erg activation curve as a parameter, we could demonstrate that TRH inhibits erg currents in a concentration as low as 10 nM, confirming the physiological role of TRH-induced erg channel modulation. Although 100 nM TRH produced a maximal effect on the endogenous erg channels, TRH was applied in a final concentration of 1 μM in all experiments with overexpressed erg channels to ensure maximal and fast activation of the signal cascade mediating the TRH effects on erg channels.

Up to now, the constituents of this signal cascade have not been completely identified (Corrette *et al.* 1995). Several studies have shown that neither the PLC–PKC pathway nor PKA activation is required for the TRH-induced erg current reduction in pituitary cells (Bauer *et al.* 1990, 1994; Barros *et al.* 1992, 1993; Schäfer *et al.* 1999; Schledermann *et al.* 2001; Gomez-Varela *et al.* 2003*b*). Different G proteins distinct from $G_{q/11}$ have been reported to be involved in the TRH-induced modulation of erg channels in clonal pituitary cells, including G_s (Bauer *et al.* 1994; Storey *et al.* 2002; Miranda *et al.* 2005). Most interestingly, a possible role for free $\beta\gamma$ subunits in this response has recently been proposed (Miranda *et al.* 2005).

Differences between the biophysical properties of rerg1a and rerg1b

Instead of the amino-terminal domain 1–376 of HERG1a, erg1b exhibits a unique N-terminal sequence of 36 amino acids. This means that erg1b lacks a large number of putative phosphorylation and possible interaction sites present in erg1a. The most apparent and best described difference between the two isoforms erg1a and erg1b are the deactivation kinetics (London *et al.* 1997; Lees-Miller *et al.* 1997). These studies have been performed on mouse and human erg channels. In the present experiments, corresponding results were obtained using the rat homologues of erg1a and erg1b, as expected by the complete identity of the unique N-terminus in rat and mouse erg1b. The much faster deactivation of erg1b compared to erg1a channels is explained by the short N-terminus of erg1b. Also the splice variant merg1a′, which lacks only the first 59 amino acids of merg1a, shows this fast deactivation (London *et al.* 1997), and the role of amino acids 2–16 in significantly slowing deactivation has been confirmed with HERG deletion mutants (Wang *et al.* 1998) and by coexpression of just this small part of the N-terminus (Wang *et al.* 2000).

The present investigation of rerg1a and rerg1b channels in parallel experiments using identical recording conditions showed that they exhibited a small, but significant difference of about 10 mV in their potential dependence of activation. These differences between the two splice variants were not found in a previous study performed in CHO cells using an external solution with elevated (40 mM) K^+ (Hirdes *et al.* 2005). Differences in the expression system are most probably not the reason for this inconsistency, because we were able to confirm our present

findings using CHO cells as the expression system (data not shown). Nevertheless, we found that considerable differences in the voltage dependence of activation of rerg1a channels could occur between sets of experiments performed with a time interval. Although less differences in erg channel properties were observed with GH_3/B_6 cells as the expression system, we took special care in the present study to perform corresponding experiments on rerg1a, rerg1b and rerg1a/1b always in parallel.

Differences in the activation time course of erg1a and erg1b channels with significantly faster activation of erg1b have been previously described (Lees-Miller *et al.* 1997; Hirdes *et al.* 2005), and these differences have been confirmed in the present study. An accelerated activation was also found for HERGΔ2–370 channels (Viloria *et al.* 2000). In contrast, HERGΔ2–354 exhibited no significant differences in the activation kinetics compared to WT-HERG, and there was even a tendency to larger time constants of activation for the mutant channels (Wang *et al.* 1998). This supposed discrepancy is explained by the finding that deletions of the proximal N-terminal as small as Δ355–373 significantly accelerate activation, suggesting opposing effects of distal and proximal regions of the N-terminus on HERG activation (Viloria *et al.* 2000). In this case, the properties of rerg1b, which lacks amino acids 1–378 of rerg1a, are only mimicked by the 'full length' deletion mutant HERGΔ2–370. Interestingly, corresponding to our findings on rerg1b channels, this mutant also exhibited a shift in the steady-state activation curve to slightly more positive potentials compared to WT HERG channels (Viloria *et al.* 2000).

The present results revealed large differences in steady-state inactivation between rerg1a and rerg1b channels. With respect to rerg1a, the inactivation curve for erg1b channels is shifted by about 50 mV to more positive potentials, resulting in considerably less inward rectification and larger outward currents. Again, there is a parallel between rerg1b and N-terminal deletion mutants. The results of these deletion experiments suggested that the presence of the N-terminus promotes and stabilizes the inactivated state, resulting in stronger inward rectification (Wang *et al.* 1998).

Properties of erg currents resulting from coexpression of rerg1a and rerg1b subunits

All electrophysiological results obtained for coexpressed rerg1a and rerg1b channel subunits point to the formation of heteromeric rat erg1 channels since no indications of significant amounts of homomeric rerg1a or rerg1b channels were observed. Evidence of functional heteromeric rerg1a/1b derived from our experiments where the dominant-negative rerg1a mutant rerg1G630S was coexpressed with rerg1b resulting in either nearly complete (ratio or 2 : 1) or strong (ratio 1 : 3) erg current reduction. In line with these electrophysiological data, coexpressed tagged rerg1a and rerg1b subunits showed always a perfectly overlapping subcellular distribution. Evidence that heteromeric erg1a/1b channels are also formed in native tissue has derived from recent studies where erg1a and erg1b subunits have been coimmunoprecipitated using human and canine cardiac tissue (Jones *et al.* 2004), tumour cells (Crociani *et al.* 2003) and mouse brain (Guasti *et al.* 2005).

When either rerg1a or rerg1b channels were expressed in GH_3/B_6 cells, rerg1a tended to a more diffuse cellular distribution compared to rerg1b channels, which were most often found in intracellular clusters. This observation raises the possibility that the relatively low rerg1b current densities do not result from generally low expression levels, but mainly from a lower percentage of functional channels in the plasma membrane. Much lower functional expression levels of erg1b compared to erg1a have also been described in the *Xenopus* oocyte expression system (London *et al.* 1997). This difference in current densities was then used to show that erg1a coexpression results in an incorporation of erg1b subunits into functional erg channels in the plasma membrane which exhibit intermediate deactivation kinetics (London *et al.* 1997). Our present results with gradually differing deactivation kinetics observed for two different ratios of injected rerg1a and rerg1b cDNAs are in line with previous results demonstrating that a small soluble N-terminal domain dose-dependently slows deactivation of HERG channels lacking the N-terminus (Wang *et al.* 2000) and demonstrate that the ratio of injected rerg cDNAs was correlated with the ratio of functionally expressed rerg1a and rerg1b channel subunits.

The present characterization of rerg1a/1b currents in GH_3/B_6 cells extends the knowledge of heteromeric erg1 current properties. The results demonstrate that rerg1a subunits dominate the voltage dependence of activation in heteromeric rerg1a/1b channels. In contrast, the steady-state inactivation curve of rerg1a/1b heteromers exhibited a more intermediate behaviour with a voltage dependence more similar to rerg1b than to rerg1a for the rerg1a : 1b cDNA ratio 1 : 3. Consequently, the amplitude of the heteromeric rerg1a/1b window conductance was much larger than that of rerg1a, although the maximum values occurred at almost the same voltage. Thus, a contribution of erg1b subunits to functional erg1 channels is suggested to result in clearly increased steady-state currents compared to homomeric erg1a channels in a voltage range close to the threshold for action potential generation and to resting membrane potential values in several cell types.

Different from the deactivation kinetics, the activation time course of the heteromeric erg channels resembled either rerg1a or rerg1b, depending on the ratio of the

injected cDNAs. Heteromeric erg channels can not only be formed by splice variants of erg1, but also by different members of the erg family (Wimmers *et al.* 2001). Corresponding to our present results, heteromeric erg channels formed by rerg1a, rerg2 and rerg3 subunits were also found to exhibit intermediate properties as well as properties dominated by one of the channel subunits (Wimmers *et al.* 2002).

Differences in the TRH-induced modulation of rerg1a and rerg1b channels

In the present study, we overexpressed rat erg1 channels in the clonal somatomammotroph GH_3/B_6 cell line and analysed their modulation by TRH as previously performed with the three different rat erg channels (Schledermann *et al.* 2001). The experiments demonstrate that rerg1a as well as rerg1b currents were effectively reduced by TRH, but they revealed also significant differences in the underlying changes in erg channel properties. In accordance with previous results (Bauer *et al.* 1990; Barros *et al.* 1998; Schledermann *et al.* 2001), the effects of TRH on rerg1a were characterized by a reduction of the maximal available current amplitude, a shift in the voltage-dependent activation to more positive potentials, an acceleration of the deactivation kinetics and a significant slowing of the activation kinetics. The TRH-induced modulation of rerg1b currents clearly differed from the TRH effects on rerg1a. The reduction of the maximal available erg current was stronger for rerg1b than for rerg1a channels, but there was no shift in the voltage dependence of activation to more positive potentials, only a marginal slowing of activation kinetics and no acceleration of the deactivation kinetics.

The reduced sensitivity of rerg1b channels to TRH parallels the effects of TRH on HERG mutants with deletions in the proximal N-terminus (especially HERGΔ326–373; Gomez-Varela *et al.* 2003a), a region which is also absent in rat or human erg1b. Nevertheless, a strong TRH-induced reduction of the maximal available erg current as found for rerg1b has not been described for the HERGΔ mutants. Although this parameter was not specifically evaluated by Gomez-Varela *et al.* (2003*a*), no significant erg current reduction is visible in the respective figures of their paper. A possible reason for this difference could be that the distal part of the N-terminus inhibits or counteracts a strong current reduction. Alternatively, the unique erg1b N-terminus could support erg current reduction by TRH. Nevertheless, it is also possible that strong erg current reduction is not produced in the heterologous *Xenopus laevis* oocyte expression system, because some constituents of the involved signal cascade(s) differ from those utilized by native pituitary TRH receptors (Barros *et al.* 1998).

Beside the similarities to HERG proximal deletion mutants, the modulation of rerg1b is reminiscent of TRH effects on rat erg3 channels. Compared to rerg1a, the TRH effects on rerg3 channels are characterized by a stronger current reduction, a smaller shift in the voltage dependence of activation and no acceleration of deactivation (Schledermann *et al.* 2001). Similar to rerg1b channels, rerg3 channels exhibit fast deactivation and reduced steady-state inactivation (Shi *et al.* 1997). A region corresponding to the proximal HERG326–373 domain is present in the sequence of rat erg3, with an amino acid identity of 65% and homology of 81% to rat erg1a.

TRH-induced modulation of heteromeric rerg1a/1b channels

Although heteromeric rerg1a/1b channels showed no clear dominance of rerg1b subunits under control conditions, rerg1b exerted a kind of 'dominant-negative' effect with respect to TRH effects on erg channel activation. Most striking is, that rerg1b subunits prevented the TRH-induced shift in the voltage dependence of activation to more positive potentials although the control values of $V_{0.5}$ were clearly determined by the presence of rerg1a subunits. Heteromeric rerg1a/1b channels also exhibited a considerably less pronounced slowing of activation kinetics than rerg1a channels. When more cDNA for rerg1b than for rerg1a was injected, the TRH-induced slowing of activation was similarly small in homomeric rerg1b and heteromeric rerg1a/1b channels. As a consequence and of possible physiological function, the effect of the TRH-induced erg1a current reduction being especially pronounced upon short depolarizations is much smaller with coexpression of erg1b.

In heteromeric rerg1a/1b channels, TRH was able to induce a significant acceleration of deactivation – an effect which was completely absent in homomeric rerg1b channels. This suggests that the TRH-induced modulation of erg channels reduces the ability of rerg1a N-termini to slow deactivation. In summary, the variable sensitivity of heteromeric rerg1a/1b channels to different TRH effects suggests that a different number of rerg1a or rerg1b N-termini is required for the establishment of the different TRH effects.

The present results concerning the biophysical properties of rerg1b and heteromeric rerg1a/1b channels as well as their modulation have implications for investigations of erg currents in every tissue expressing or coexpressing erg1b. In addition to the heart, erg1b transcripts have been detected in brain, lung and muscle (Lees-Miller *et al.* 1997; London *et al.* 1997). Recently, erg1b coexpression and coassembly with erg1a on the protein level have been described in mouse brain (Guasti *et al.* 2005), and the coexpression of erg1b mRNA

transcripts with other erg transcripts on the single cell level is shown in raphe neurons, which exhibit relatively fast activating and deactivating endogenous erg currents (Hirdes *et al.* 2005). Coexpression of erg1a and erg1b protein has also been demonstrated in different tumour cells. In these cells, cell-cycle-dependent changes in the protein level were found which were more pronounced for erg1a than for erg1b, resulting in varying ratios of erg1a to erg1b subunits (Crociani *et al.* 2003).

As shown in the present study, the ratio of rerg1a to rerg1b expression determines the level of steady-state erg current at potentials close to the resting membrane potential as well as the gating kinetics of heteromeric rerg1a/1b channels. In addition, a potential modulation of erg channels by hormones or transmitters acting through metabotropic receptors would be altered concomitantly with the relative contribution of the two erg1 isoforms to the subunit composition of the erg channels.

In the mammalian brain, TRH acts through two different G protein-coupled receptors which exhibit a partially overlapping distribution (Sun *et al.* 2003). So far, no differences in the activated signal cascades have been reported. Nevertheless, future experiments have to clarify whether the present results obtained with TRH-R1, which is highly expressed not only in the pituitary, but also in neuroendocrine brain regions, the autonomic nervous system and visceral brainstem regions, are valid also for TRH-R2 with respect to the differences in the TRH-induced modulation of homo- and heteromeric rerg1a/rerg1b channels.

References

Barros F, Delgado LM, del Camino D & de la Peña P (1992). Characteristics and modulation by thyrotropin-releasing hormone of an inwardly rectifying K^+ current in patch-perforated GH_3 anterior pituitary cells. *Pflugers Arch* **422**, 31–39.

Barros F, Gómez-Varela D, Viloria CG, Palomero T, Giráldez T & de la Peña P (1998). Modulation of human erg K^+ channel gating by activation of a G-protein-coupled receptor and protein kinase C. *J Physiol* **511**, 333–346.

Barros F, Mieskes G, del Camino D & de la Peña P (1993). Protein phosphatase 2A reverses inhibition of inward rectifying K^+ currents by thyrotropin-releasing hormone in GH_3 pituitary cells. *FEBS Lett* **336**, 433–439.

Bauer CK (1998). The erg inwardly rectifying K^+ current and its modulation by thyrotropin-releasing hormone in giant clonal rat anterior pituitary cells. *J Physiol* **510**, 63–70.

Bauer CK, Davison I, Kubasov I, Schwarz JR & Mason WT (1994). Different G proteins are involved in the biphasic response of clonal rat pituitary cells to thyrotropin-releasing hormone. *Pflugers Arch* **428**, 17–25.

Bauer CK, Engeland B, Wulfsen I, Ludwig J, Pongs O & Schwarz JR (1998). RERG is a molecular correlate of the inward-rectifying K current in clonal rat pituitary cells. *Receptors Channels* **6**, 19–29.

Bauer CK, Meyerhof W & Schwarz JR (1990). An inward-rectifying K^+ current in clonal rat pituitary cells and its modulation by thyrotrophin-releasing hormone. *J Physiol* **429**, 169–189.

Bauer CK, Schäfer R, Schiemann D, Reid G, Hanganu I & Schwarz JR (1999). A functional role of the erg-like inward-rectifying K^+ current in prolactin secretion from rat lactotrophs. *Mol Cell Endocrinol* **148**, 37–45.

Bauer CK & Schwarz JR (2001). Physiology of EAG K^+ channels. *J Membr Biol* **182**, 1–15.

Corrette BJ, Bauer CK & Schwarz JR (1995). Electrophysiology of anterior pituitary cells. In *The Electrophysiology of Neuroendocrine Cells*, ed. Scherübl H & Hescheler J, pp. 101–143. CRC Press, Boca Raton, FL, USA.

Corrette BJ, Bauer CK & Schwarz JR (1996). An inactivating inward-rectifying K current present in prolactin cells from the pituitary of lactating rats. *J Membr Biol* **150**, 185–195.

Crociani O, Guasti L, Balzi M, Becchetti A, Wanke E, Olivotto M, Wymore RS & Arcangeli A (2003). Cell cycle-dependent expression of HERG1 and HERG1B isoforms in tumor cells. *J Biol Chem* **278**, 2947–2955.

Gómez-Varela D, Barros F, Viloria CG, Giráldez T, Manso DG, Dupuy SG, Miranda P & de la Peña P (2003*a*). Relevance of the proximal domain in the amino-terminus of HERG channels for regulation by a phospholipase C-coupled hormone receptor. *FEBS Lett* **535**, 125–130.

Gómez-Varela D, Giráldez T, de la Peña P, Dupuy SG, García-Manso D & Barros F (2003*b*). Protein kinase C is necessary for recovery from the thyrotropin-releasing hormone-induced r-ERG current reduction in GH_3 rat anterior pituitary cells. *J Physiol* **547**, 913–929.

Guasti L, Cilia E, Crociani O, Hofmann G, Polvani S, Becchetti A, Wanke E, Tempia F & Arcangeli A (2005). Expression pattern of the ether-a-go-go-related (ERG) family proteins in the adult mouse central nervous system: evidence for coassembly of different subunits. *J Comp Neurol* **491**, 157–174.

Hirdes W, Schweizer M, Schuricht KS, Guddat SS, Wulfsen I, Bauer CK & Schwarz JR (2005). Fast erg K^+ currents in rat embryonic serotonergic neurones. *J Physiol* **564**, 33–49.

Horn R & Marty A (1988). Muscarinic activation of ionic currents measured by a new whole-cell recording method. *J General Physiol* **92**, 145–159.

Jones EM, Roti Roti EC, Wang J, Delfosse SA & Robertson GA (2004). Cardiac I_{Kr} channels minimally comprise hERG1a and 1b subunits. *J Biol Chem* **279**, 44690–44694.

Kirchberger NM, Wulfsen I, Schwarz JR & Bauer CK (2005). Biophysical properties and modulation of erg1a, erg1b and heteromeric erg1 K^+ channels. *Pflugers Arch* **449** (Suppl.), S83.

Lees-Miller JP, Kondo C, Wang L & Duff HJ (1997). Electrophysiological characterization of an alternatively processed ERG K^+ channel in mouse and human hearts. *Circ Res* **81**, 719–726.

London B, Trudeau MC, Newton KP, Beyer AK, Copeland NG, Gilbert DJ *et al.* (1997). Two isoforms of the mouse ether-a-go-go-related gene coassemble to form channels with properties similar to the rapidly activating component of the cardiac delayed rectifier K^+ current. *Circ Res* **81**, 870–878.

Miranda P, Giráldez T, de la Peña P, Manso DG, Alonso-Ron C, Gómez-Varela D, Domínguez P & Barros F (2005). Specificity of TRH receptor coupling to G-proteins for regulation of ERG K^+ channels in GH_3 rat anterior pituitary cells. *J Physiol* **566**, 717–736.

Ohya S, Horowitz B & Greenwood IA (2002). Functional and molecular identification of ERG channels in murine portal vein myocytes. *Am J Physiol Cell Physiol* **283**, C866–C877.

Papa M, Boscia F, Canitano A, Castaldo P, Sellitti S, Annunziato L & Taglialatela M (2003). Expression pattern of the ether-a-gogo-related (ERG) K^+ channel-encoding genes ERG1, ERG2, and ERG3 in the adult rat central nervous system. *J Comp Neurol* **466**, 119–135.

Saganich MJ, Machado E & Rudy B (2001). Differential expression of genes encoding subthreshold-operating voltage-gated K^+ channels in brain. *J Neurosci* **21**, 4609–4624.

Sanguinetti MC, Curran ME, Spector PS & Keating MT (1996). Spectrum of HERG K^+-channel dysfunction in an inherited cardiac arrhythmia. *Proc Natl Acad Sci U S A* **93**, 2208–2212.

Sanguinetti MC, Jiang C, Curran ME & Keating MT (1995). A mechanistic link between an inherited and an acquired cardiac arrhythmia: HERG encodes the I_{Kr} potassium channel. *Cell* **81**, 299–307.

Sanguinetti MC & Jurkiewicz NK (1990). Two components of delayed rectifier K^+ current: differential sensitivity to block by class III antiarrhythmic agents. *J General Physiol* **96**, 195–215.

Schäfer R, Wulfsen I, Behrens S, Weinsberg F, Bauer CK & Schwarz JR (1999). The erg-like potassium current in rat lactotrophs. *J Physiol* **518**, 401–416.

Schledermann W, Wulfsen I, Schwarz JR & Bauer CK (2001). Modulation of rat erg1, erg2, erg3 and HERG K^+ currents by thyrotropin-releasing hormone in anterior pituitary cells via the native signal cascade. *J Physiol* **532**, 143–163.

Schönherr R & Heinemann SH (1996). Molecular determinants for activation and inactivation of HERG, a human inward rectifier potassium channel. *J Physiol* **493**, 635–642.

Shi WM, Wymore RS, Wang HS, Pan ZM, Cohen IS, McKinnon D & Dixon JE (1997). Identification of two nervous system-specific members of the erg potassium channel gene family. *J Neurosci* **17**, 9423–9432.

Shibasaki T (1987). Conductance and kinetics of delayed rectifier potassium channels in nodal cells of the rabbit heart. *J Physiol* **387**, 227–250.

Smith PL, Baukrowitz T & Yellen G (1996). The inward rectification mechanism of the HERG cardiac potassium channel. *Nature* **379**, 833–836.

Spector PS, Curran ME, Zou A, Keating MT & Sanguinetti MC (1996). Fast inactivation causes rectification of the I_{Kr} channel. *J General Physiol* **107**, 611–619.

Storey NM, O'Bryan JP & Armstrong DL (2002). Rac and Rho mediate opposing hormonal regulation of the ether-a-go-go-related potassium channel. *Curr Biol* **12**, 27–33.

Sturm P, Wimmers S, Schwarz JR & Bauer CK (2005). Extracellular potassium effects are conserved within the rat erg K^+ channel family. *J Physiol* **564**, 329–345.

Sun Y, Lu X & Gershengorn MC (2003). Thyrotropin-releasing hormone receptors – similarities and differences. *J Mol Endocrinol* **30**, 87–97.

Trudeau MC, Warmke JW, Ganetzky B & Robertson GA (1995). HERG, a human inward rectifier in the voltage-gated potassium channel family. *Science* **269**, 92–95.

Viloria CG, Barros F, Giràldez T, Gómez-Varela D & de la Peña P (2000). Differential effects of amino-terminal distal and proximal domains in the regulation of human *erg* K^+ channel gating. *Biophys J* **79**, 231–246.

Wang S, Liu S, Morales MJ, Strauss HC & Rasmusson RL (1997). A quantitative analysis of the activation and inactivation kinetics of *HERG* expressed in *Xenopus* oocytes. *J Physiol* **502**, 45–60.

Wang J, Myers CD & Robertson GA (2000). Dynamic control of deactivation gating by a soluble amino-terminal domain in HERG K^+ channels. *J General Physiol* **115**, 749–758.

Wang J, Trudeau MC, Zappia AM & Robertson GA (1998). Regulation of deactivation by an amino terminal domain in *human ether-à-go-go-related gene* potassium channels. *J General Physiol* **112**, 637–647.

Warmke JW & Ganetzky B (1994). A family of potassium channel genes related to *eag*. *Drosophila* and mammals. *Proc Natl Acad Sci U S A* **91**, 3438–3442.

Weinsberg F, Bauer CK & Schwarz JR (1997). The class III antiarrhythmic agent E-4031 selectively blocks the inactivating inward-rectifying potassium current in rat anterior pituitary tumor cells (GH_3/B_6 cells). *Pflugers Arch* **434**, 1–10.

Wimmers S, Bauer CK & Schwarz JR (2002). Biophysical properties of heteromultimeric erg K^+ channels. *Pflugers Arch* **445**, 423–430.

Wimmers S, Wulfsen I, Bauer CK & Schwarz JR (2001). Erg1, erg2 and erg3 K channel subunits are able to form heteromultimers. *Pflugers Arch* **441**, 450–455.

Wulfsen I, Hauber HP, Schiemann D, Bauer CK & Schwarz JR (2000). Expression of mRNA for voltage-dependent and inward-rectifying K channels in GH_3/B_6 cells and rat pituitary. *J Neuroendocrinol* **12**, 263–272.

Acknowledgements

We thank C. Reißmann, I. Blank and W. Krüger for technical help, and the Deutsche Forschungsgemeinschaft for financial support (GK255, SFB444). The data presented here are part of the thesis of N.K.